

ChemComm

Accepted Manuscript



This is an *Accepted Manuscript*, which has been through the Royal Society of Chemistry peer review process and has been accepted for publication.

Accepted Manuscripts are published online shortly after acceptance, before technical editing, formatting and proof reading. Using this free service, authors can make their results available to the community, in citable form, before we publish the edited article. We will replace this *Accepted Manuscript* with the edited and formatted *Advance Article* as soon as it is available.

You can find more information about *Accepted Manuscripts* in the [Information for Authors](#).

Please note that technical editing may introduce minor changes to the text and/or graphics, which may alter content. The journal's standard [Terms & Conditions](#) and the [Ethical guidelines](#) still apply. In no event shall the Royal Society of Chemistry be held responsible for any errors or omissions in this *Accepted Manuscript* or any consequences arising from the use of any information it contains.

COMMUNICATION

Fast detection of nitroaromatics using phosphonate pyrene motifs as dual chemosensors

Cite this: DOI: 10.1039/x0xx00000x

N. Venkatramiah,^{a,b} Ana. D. G. Firmino,^{a,b} Filipe A. Almeida Paz^{b*} and João P. C. Tomé^{a,c*}Received 00th January 2012,
Accepted 00th January 2012

DOI: 10.1039/x0xx00000x

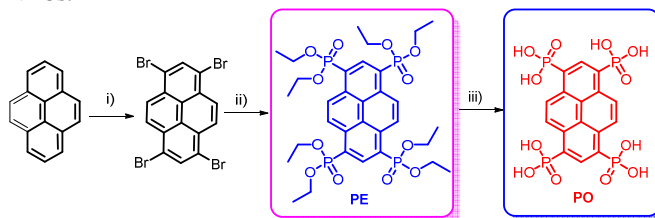
www.rsc.org/

A new class of dual fluorescent chemosensors for nitroaromatic compounds (NACs) based on phosphonated pyrene derivatives is reported, showing high selectivity towards trinitrotoluene (TNT). The strong intermolecular interactions (π - π stacking and hydrogen bonding) allow high fluorescence quenching with visual detection in short response times.

Rapid screening of explosive nitroaromatic compounds (NACs) in pre and post-blast debris is of high importance for both environmental and security reasons.¹ Current detection methods are cumbersome, require pre-treatment of the samples and susceptible to interference from other compounds, and suffer from low sensitivity.² Fluorescence studies have received great attention in this field due to their intrinsic high sensitivity (even at the atto-gram level) and rapid detection by photo induced electron transfer from the excited state of the donor to NACs (acceptors).^{3,4} A considerable number of fluorescent probes have been designed for this purpose including a wide variety of functional groups.⁵ It remains, nevertheless, a great challenge to find new materials that could improve the selectivity and sensitivity towards the detection of NACs.⁶

Polycyclic π -conjugated systems, such as pyrene, have an intrinsic high fluorescent quantum yield.⁷ The presence of the large conjugated backbone is additionally highly beneficial to bind to aromatic rings through π - π interactions.⁸ Covalent attachment of pyrene derivatives with polymer networks and physical encapsulation with nanoparticles were used for the detection of NACs based on the behaviour of monomer to excimer emission.⁹ The formation of stable and pure excimer emission is a challenging task because of its high sensitivity to the guest molecules. In this communication, we report the design and simple (and fast) preparation of two pyrene derivatives covalently functionalized with phosphonate groups (protected and hydrolyzed, **PE** and **PO** respectively; Scheme 1). We have investigated their potential utility as chemosensors in the detection of NACs (Fig. S1, ESI[†]), in solution and solid state methods. These molecules were designed based on the principle that the P=O functional group reduces the lowest unoccupied molecular orbital (LUMO) energy level of the resulting molecule and, consequently, facilitates the electron inoculation to electron deficient NACs. While the phosphoryl groups

can limit molecular aggregation (due to steric hindrance), the unprotected hydroxyl groups further act as donor/receptors in strong intermolecular hydrogen bonding interactions with electron-deficient NACs.



i) Br₂, Nitrobenzene, 120 °C, 4 h; ii) P(OC₂H₅)₃, Pd(PPh₃)₄, 230 °C, 100 PSI, 120 W, 45 min, iii) 6M HCl, 80 °C, 20 h

Scheme 1. Synthetic route for the preparation of phosphonated pyrene derivatives.

PE was easily prepared in quantitatively yields (*ca.* 95%) by a palladium-catalysed cross-coupling reaction under microwave irradiation at 230 °C for 45 min. Acid hydrolysis was carried out using a 6M HCl solution at 80 °C yields the pyrene tetraphosphonic acid (**PO**) in quantitative yields. The molecular structures of the final compounds were investigated in solution using a myriad of techniques: ¹H, ³¹P, ¹³C NMR and MALDI-TOF MS (Figs. S2-S12, ESI[†]). ¹H NMR of **PE** and **PO** reveals the presence of a set of singlet peak corresponding to the four protons of the 4,5,9,10 positions of pyrene (9.19 and 8.53 ppm respectively), while the protons at the 2,7 positions appear as triplets due to long range phosphorous-hydrogen coupling (for **PE**: 9.23- 9.33 ppm with ⁵J_{HP} = 30 Hz; for **PO**: 8.58-8.60 ppm with ⁵J_{HP} = 6 Hz). In the aliphatic region of **PE** clearly appear the resonances corresponding to the ethoxy groups at δ 1.38 (-CH₃) and 4.27 (-CH₂) ppm, while in **PO**, these signals disappear confirming the full deprotection of their hydroxyl groups.³¹P NMR spectra shows one set of triplet peaks centred at 17 ppm (²J_{HP} = 12.1 Hz) and 13.5 ppm (⁵J_{HP} = 14.5 Hz in D₂O) for **PE** and **PO**, respectively. The MALDI-TOF MS results confirm the proposed structures. The absorption spectra of **PE** and **PO** in methanol exhibit two major bands centred at *ca.* 283 nm and 375 nm and attributed to the electronic transitions between the S₀→S₂ and S₀→S₁ energy levels (Fig. 2a). The emission spectra are typical of the monomeric form of pyrene with emission maxima centred at *ca.* 387 (Fig. 2b), with lifetimes of 3.74 ns (**PE**) and 3.42 ns (**PO**) (Fig. 2c), and optical

band gaps of 3.10 and 3.01 eV, respectively. The absorption and emission spectra in different solvents was shown in Fig. S13-14, ESI[†]. Contrasting with the absorption spectra in solution, the emission of thin films show broad emission bands at *ca.* 505 nm (**PE**) and 515 nm (**PO**) with Stokes shift of 132 nm and 140 nm indicating formation of excimer in the solid state. The excimer emission of **PE** and **PO** was found to be $\sim 45 \pm 5$ nm higher than that of pyrene.^{9d} The inset in Fig. 2b shows comparative the emission behaviour of **PE** and **PO** in solution and in thin films under UV light ($\lambda_{\text{ex}}=365$ nm). While the fluorescence quantum yields (Φ_{F}) of **PE** and **PO** in solution are *ca.* 36% and 22%, a notable decrease to *ca.* 3.2% and 1.7% was observed for the solid state. The photophysical properties of **PE** and **PO**, both in solution and solid state are summarized in Table S1, ESI[†]. Fig. 2d depicts the spectrofluorimetric addition of **PO** with different concentrations of TNT in methanol while exciting at 330 nm. As expected the fluorescence intensity gradually depletes, showing *ca.* 82% and 91% quenching effect for **PE** and **PO** with a limit of detection (LOD) in the range of 2-14 ppb; for TNP the analogous results for **PE** and **PO** are 51% and 74%, respectively (Fig. S15, ESI[†]). The high quenching efficiency of **PO** emission with the addition of TNT is attributed to strong π - π interactions between the quencher and **PO** through a photo-induced electron transfer (PET).

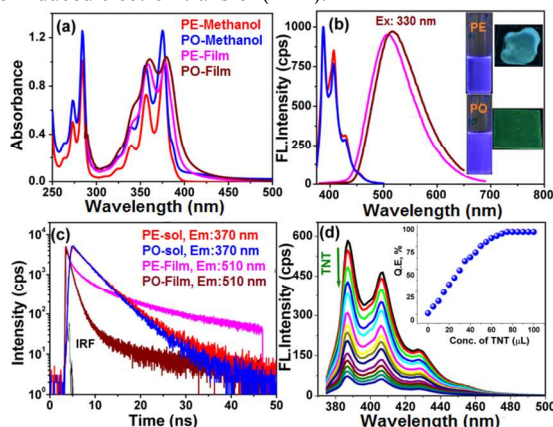


Fig. 2 (a) Absorption (b) emission spectra and (c) fluorescence lifetime decay of **PE** and **PO** in methanol and in thin films. The inset in Fig. 2b shows the emission behaviour of **PE** and **PO** in solution and in the solid state under UV light at 365 nm. (d) Emission spectra of **PO** upon gradual addition of different concentrations of TNT at $\lambda_{\text{ex}}=330$ nm. The inset shows the trend in the quenching efficiency of **PO** at different concentrations of TNT.

In addition to π - π interactions, **PO** should also exhibit strong intermolecular hydrogen bonding interactions between the hydroxyl groups of the phosphonic acids and nitro groups of the quencher, resulting in an enhanced quenching efficiency in comparison to that observed for parent **PE** (Fig. S16, ESI[†]). Non-aromatic analytes such as nitromethane (NM) showed a lower quenching response mainly because of its inability to interact via π - π interactions. We further emphasize that addition of other NACs and volatile organic compounds did not produce any sensible changes in the fluorescence intensity. It further evidences that both **PE** and **PO** exhibit high selectivity towards TNT and TNP in methanol (Figs. S15-16, ESI[†]). The visual modification of the strong blue fluorescence emission of **PE** and **PO** was monitored by adding different NACs. Both **PE** and **PO** show turn-off fluorescence behaviour in the presence of TNT and TNP (Fig. S17, ESI[†]). Fig. 3a shows the comparison of the quenching efficiency of **PE** and **PO** with different nitroaromatics: TNP has a moderate quenching efficiency while TNT show significantly enhanced selectivity for **PO** rather than for **PE** (Fig. S18, ESI[†]). The fluorescence attenuation of **PO** against NACs at different concentrations was quantitatively evaluated using Stern-

Volmer (SV) plots (Fig. 3b). The SV plots indicate high binding constants for TNT ($K_{\text{sv}}=8.4 \times 10^4 \text{ M}^{-1}$) and TNP ($K_{\text{sv}}=3.6 \times 10^4 \text{ M}^{-1}$; Table S2, ESI[†]). They further evidence linear response behaviour upon addition of TNT at low concentrations, with a positive upward deviation indicating the formation of static and dynamic quenching effects. **PE** shows, however, a $K_{\text{sv}}=6.6 \times 10^4 \text{ M}^{-1}$ for TNT and $K_{\text{sv}}=2.9 \times 10^4 \text{ M}^{-1}$ for TNP and exhibit linear SV plots on addition of different NACs. This ascribed due to static quenching phenomena (Fig. S19, ESI[†]). We note that the rate constants of these phosphonate pyrene derivatives were found to be higher than those of related derivatives employed for detection of NACs.¹⁰ The obvious modifications in the UV-Vis spectra of **PO** upon addition of TNT confirmed the formation of complexes in the ground state (Fig. S20, ESI[†]). Further, time-resolved fluorescence emission (Fig. S21, ESI[†]) reveals a change in the lifetime of **PO** upon addition of different concentrations of TNT, ultimately confirming the quenching of the excited state (Table S3, ESI[†]).

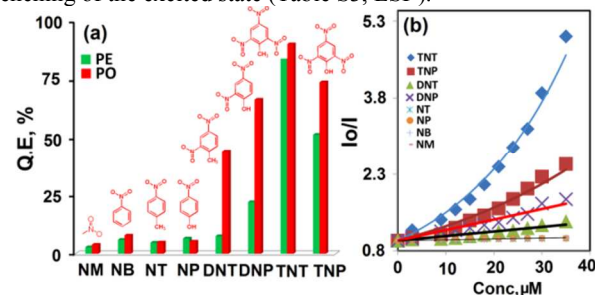


Fig. 3 (a) Quenching efficiency of **PE** and **PO** for various NACs. (b) Stern-Volmer (SV) plot of **PO** treated with different NACs at different concentrations.

The DFT optimized structures of **PE** and **PO** and its adducts with TNT and TNP was carried out using the B3LYP/6-31g* basis set in Gaussian 03 package (Figs. S22-24, ESI[†]). The phosphonate groups of **PO** and **PE** reveal a decrease in the LUMO energy level in comparison with that of pyrene (Fig. S25, ESI[†]). The electron density of the HOMO orbitals of **PO**-TNT and **PE**-TNT adducts are localized on the pyrene backbone; the LUMO orbitals localized on TNT are strong evidence for an efficient charge transfer process occurring between the higher energy state of the pyrene phosphonates and the lower-energy state of NACs (Fig. S26, ESI[†]). The **PO**-TNT adduct is energetically more stable than **PE**-TNT by *ca.* 3.23 kcal mole⁻¹. Cyclic-voltametric studies with Fc/Fc+ couple showed one reversible reduction half wave potential at ($E_{1/2}$) -1.05 V, -1.08 V for **PE** and **PO** (Fig. S27, ESI[†]). The LUMO energy of **PO** (-3.43 eV) is close to the LUMO of TNT (-3.7 eV), favouring electron transfer.

To gain more insight into the mechanism of sensing, we have performed ¹H NMR titration with TNT (Figs. S28-32, ESI[†]). Upon a gradual addition of TNT at different mole ratios to **PE**, the singlet and triplet peaks are shifted towards the up field region. The degree of the shift was, however, greater for the singlet peak ($\Delta\delta = -0.07$ ppm) which is an indication of π - π stacking (Fig. S29, ESI[†]). Similar results were obtained for **PO** treated with different concentrations of TNT (Figs. S30-32, ESI[†]): The -OH protons of **PO** at $\delta = 4.24$ ppm broaden with small up-field shift upon addition of TNT, evidencing the formation of hydrogen bonds between the -OH and -NO₂ groups (Fig. S32, ESI[†]). A possible mode of interaction between **PO** and TNT is illustrated in Fig. S33, ESI[†]. The sensing performance of thin films of **PE** and **PO** were tested using saturated vapours of the herein investigated NACs. Fig. 4a shows the time-dependent fluorescence emission spectra of **PO** exposed to saturated vapours of TNT (*ca.* 10 ppb) with an excitation at $\lambda_{\text{ex}}=370$ nm.^{1b} The fluorescence intensity of **PO** film decreases significantly, showing a 30% quenching at 517 nm in 30 sec of exposure. A fluorescence

quenching of 93% was achieved within 180 sec of exposure time, reaching the equilibrium for elapsed time of exposure. The inset in Fig. 4a depicts the change in the emission intensity as a function of time: PE shows a 24% and 86% quenching effect in 30 and 360 sec of exposure time, respectively. Fig. 4b shows the variation in the quenching efficiency of PE and PO films to saturated vapours of different NACs. These results show that both PE and PO films are highly efficient and selective towards sensing TNT. The other tested NACs exhibit, however, a much less quenching efficiency: for example, for TNP only a *ca.* 56% quenching effect in 270 sec of exposure was observed. The variation in the quenching efficiency arises from a combination of: i) the variation in the vapour pressure of NACs; ii) exergonicity (ΔG°) of electron transfer between pyrene motifs and TNT with an effective binding strength; iii) easy diffusion on the surface. This study was extended to the vapours of other molecules such as toluene, DDQ and amine derivatives. We have observed no significant variation in the emission pattern, further evidencing the high selectivity of PO towards TNT (Fig. S35, ESI[†]). Fig. 4d depicts the SEM images of the pyrene derivatives on the glass surface, showing that PE leads to a layer-like film while PO promotes the self-assembly of fibres.

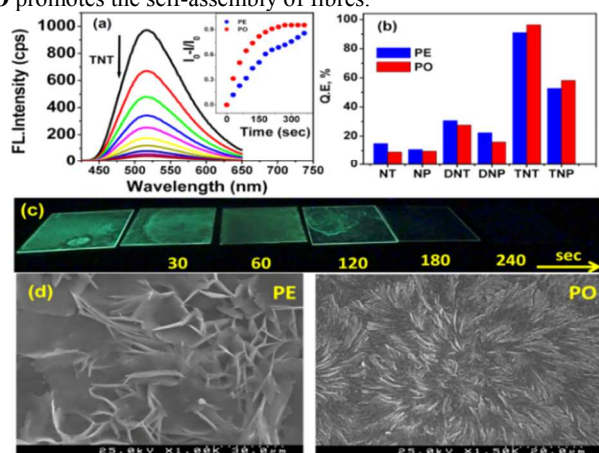


Fig. 4 (a) Time-dependent emission spectra of a PO thin film upon exposure to saturated vapours of TNT. The inset shows the fluorescence quenching of PE and PO as a function of time. (b) Quenching efficiency of PE and PO films to the saturated vapours of NACs. (c) Photograph of PO thin film under UV light at 365 nm before and after exposure to the TNT vapours at different time intervals. (d) SEM image of PE and PO thin films.

Aiming towards practical application of the herein developed materials, the reversibility of the sensing process was further examined by exposing the films to the saturated vapours of TNT for 120 sec. The emission spectrum of the film was collected before and after exposure to the TNT vapours. The recovery of excimer emission intensity was significant indicating a high photo-stability of the films after 8 cycles (Fig. S36, ESI[†]). Further, portable paper-based test strips allow a simple and low cost protocol for on-site instant detection of TNT (Fig. S37, ESI[†]).

In summary, we have developed novel sensor compounds based on phosphonate groups (protected and deprotected) appended to a pyrene core. This system acts as a dual chemosensor for the fast detection of TNT: as a monomer in solution and as a stable excimer in the solid state. The phosphonate groups attached to the pyrene decrease the LUMO energy, with the PO exhibiting simultaneously π - π stacking and strong hydrogen bonding interactions between the phosphonic acid and the nitro groups of TNT, ultimately enhancing sensitivity and selectivity. The formation of porous and fibril-type layer of thin films of PO and PE open the possibility of fabricating promising, photo-stable and highly responsive materials towards the detection of NACs. We believe that the phosphonic acid groups can greatly facilitate the construction of next-generation materials for the

detection of NACs, some of them based on metallic centres (such as metal-organic frameworks), while simultaneously providing new avenues to design more eco-friendly heterogeneous catalysts for degradation of toxic NACs.

Acknowledgement

We would like to thank Fundação para a Ciência e a Tecnologia (FCT, Portugal), the European Union, QREN, FEDER through the COMPETE program, QOPNA research unit (project PEst-C/UI0062/2013; FCOMP-01-0124-FEDER-037296) and CICECO associated Lab (PEst-C/CTM/LA0011/2013; FCOMP-01-0124-FEDER-037271) for their general funding scheme. We further wish to thank FCT for funding the R&D project (EXPL/CTM-NAN/0013/2013; FCOMP-01-0124-FEDER-041282). The authors acknowledge FCT for the post-doctoral and doctoral grants SFRH/BPD/79000/2011 (to NVR) and SFRH/BD/84495/2012 (to ADGF). We thank to Prof. Satish Patil, SSCU, Indian Institute of Science (IISc), Bangalore for useful discussions.

Notes and references

^aDepartment of Chemistry, QOPNA, University of Aveiro, 3810-193 Aveiro, Portugal. E-mail: jtome@ua.pt; Fax: +351 234370084; Tel: +351 234370342.

^bDepartment of Chemistry, CICECO, University of Aveiro, 3810-193 Aveiro, Portugal. E-mail: filipe.paz@ua.pt; Fax: +351 234401470; Tel: +351 234401418.

^cDepartment of Organic Chemistry, Ghent University, B-9000 Gent, Belgium.

[†]Electronic Supplementary Information (ESI) available: Synthesis, UV-Vis and fluorescence quenching studies with various studied analytes, both in solution and in the solid state, NMR and DFT studies. For ESI, other electronic format See DOI: 10.1039/b000000x/

- V. K. Balakrishnan, A. Halsz, J. Hawari, *Environ. Sci. Technol.*, 2003, **37**, 1838; (b) D. T. McQuade, A. E. Pullen and T. M. Swager, *Chem. Rev.*, 2000, **100**, 2537; (c) M. E. Germain and M. J. Knapp, *Chem. Soc. Rev.*, 2009, **38**, 2543.
- (a) G. He, H. Peng, T. Liu, M. Yang, Y. Zhang and Y. Fang, *J. Mater. Chem.*, 2009, **19**, 7347; (b) I. A. Popov, H. Chen, O. N. Kharybin, E. N. Nikolaev and R. G. Cooks, *Chem. Commun.*, 2005, 1953; (c) K. L. Diehl and E. V. Anslyn, *Chem. Soc. Rev.*, 2013, **42**, 8596; (d) Y. Salinas, R. M. Máñez, M. D. Marcos, F. Sancenón, A. M. Costero, M. Parra and S. Gil, *Chem. Soc. Rev.*, 2012, **41**, 1261.
- (a) K. K. Kartha, S. S. Babu, S. Srinivasan, A. Ajayaghosh, *J. Am. Chem. Soc.*, 2012, **134**, 4834; (b) V. Bhalla, S. Pramanik and M. Kumar, *Chem. Commun.*, 2013, **49**, 895.
- (a) J. Wu, W. Liu, J. Ge, H. Zhang and P. Wang, *Chem. Soc. Rev.*, 2011, **40**, 3483; (b) S. J. Toal and W. C. Trogler, *J. Mater. Chem.*, 2006, **16**, 2871; (c) S. W. Thomas III, G. D. Joly, and T. M. Swager, *Chem. Rev.*, 2007, **107**, 1339.
- (a) L. Zhao, Y. Chu, C. He and C. Duan, *Chem. Commun.*, 2014, **50**, 3467; (b) P. Wu and X. Ping Yan, *Chem. Soc. Rev.*, 2013, **42**, 5489.
- (a) G. V. Zyryanov, M. A. Palacios, P. Anzenbacher, *Org. Lett.*, 2008, **10**, 3681; (b) N. Venkatramaiah, Shiv Kumar and Satish Patil, *Chem. Commun.*, 2012, **48**, 5007; (c) Y. H. Lee, H. Liu, J. Y. Lee, S. H. Kim, S. K. Kim, J. L. Sessler, Y. Kim and J. S. Kim, *Chem. Eur. J.*, 2010, **16**, 5895.
- (a) M. Zhu and C. Yang, *Chem. Soc. Rev.*, 2013, **42**, 4963; (b) T. M. Figueira-Duarte, K. Müllen, *Chem. Rev.*, 2011, **111**, 7260.
- (a) S. M. Bromfield, E. Wilde and David K. Smith, *Chem. Soc. Rev.*, 2013, **42**, 9184; (b) N. Venkatramaiah, S. Kumar and S. Patil, *Chem. Eur. J.*, 2012, **12**, 14745; (c) J. Huang, Y. R. Wu, Y. Chen, Z. Zhu, X. H. Yang, C. Y. J. Yang, K. M. Wang, W. H. Tan, *Angew. Chem., Int. Ed.*, 2011, **50**, 401.
- (a) K. Sarkar, Y. Salinas, I. Campos, R. Martínez-Máñez, M. D. Marcos, F. Sancenón and P. Amorós, *ChemPlusChem.*, 2013, **78**, 684; (b) Y. Salinas, A. Agostini, É. Pérez-Estevé, R. Martínez-Máñez, F. Sancenón, M. D. Marcos, J. Soto, A. M. Costero, S. Gil, M. Parrae and P. Amorós, *J. Mater. Chem. A*, 2013, **1**, 3561; (c) C. E. Agudelo-Morales, R. E. Galian and J. Pérez-Prieto, *Anal. Chem.*, 2012, **84**, 8083; (d) G. Birlık Demirel, B. Daglar and M. Bayindir, *Chem. Commun.*, 2013, **49**, 6140.
- (a) P. Beyazkılıç, A. Yildirim and M. Bayindir, *ACS Appl. Mater. Interfaces.*, 2014, **6**, 4997.